JOURNAL OF PROPULSION AND POWER
Vol. 17, No. 3, May–June 2001

Theoretical Performance of Frictionless Magnetohydrodynamic-Bypass Scramjets

Chul Park* and David Bogdanoff†
Eloret Corporation, Sunnyvale, California 94087
and
Unmeel B. Mehta‡
NASA Ames Research Center, Moffett Field, California 94035-1000

Theoretical performance calculation is made of a scramjet propulsion system incorporating a magnetohydrodynamic (MHD)-energy-bypass scheme. The MHD generator upstream of the combustion chamber slows down the flow so that the Mach number at the entrance of the combustion chamber is kept below a specified value. The MHD accelerator downstream of the combustion chamber accelerates the flow, expending the electrical power produced by the generator. The flow is seeded with potassium or cesium, and the MHD devices operate as Faraday machines. Friction is neglected, and chemical equilibrium is assumed everywhere except in the nozzle downstream of the freezing point. The calculation shows that the MHD-bypass scheme can improve specific impulse over that of a conventional scramjet at flight speeds over 3.5 km/s. At speeds below about 6 km/s, the calculated specific impulse can be higher than that of a typical rocket engine. Consequently, the MHD-bypass scheme can extend the operational range or improve the performance of a conventional scramjet engine.

Nomenclature

A	=	cross-sectional area, m^2
B	=	applied magnetic field, T
E	=	voltage gradient, V/m
H	=	total enthalpy ($h + u^2/2$), J/kg
h	=	static enthalpy, J/kg
j	=	electrical current density, A/m^2
p	=	pressure, Pa
q	=	flight dynamic pressure, atm
u	=	axial velocity, m/s
V	=	flight velocity, m/s
x, y	=	axial and transverse coordinates, m
α	=	load factor (E_y/uB)
δ	=	compression ramp angles, deg
ρ	=	flow density, kg/m^3
σ	=	electrical conductivity, mho/m
τ	=	average collision time, s
ϕ	=	fuel equivalence ratio

Subscripts

ci	=	combustion chamber entrance
1	=	MHD generator
2	=	MHD accelerator

Introduction

FOR futuristic high-speed transportation the supersonic-combustion-ramjet, i.e., scramjet, propulsion system has been studied over many years. At least theoretically scramjet-propelled vehicles can fly to a high hypersonic Mach number with a fuel consumption rate comparable to that achieved at low speeds. One major problem in the scramjet system in reaching high-flight Mach numbers is the difficulty in mixing of air with fuel at the molecular level within a short distance at high local Mach numbers. The major issue is the combustor length required for complete mixing of air and fuel. This issue is significant because the specific impulse produced by the combustor decreases rapidly as the distance for complete mixing increases. One solution of this problem is to lower the combustor entrance Mach number with a magnetohydrodynamic (MHD)-energy-bypass scheme.[1]

In Fig. 1 the specific impulses obtainable by an ideal frictionless scramjet system are shown for the case where the Mach number at the combustion chamber entrance M_{ci} is unlimited and for cases where it is limited to 2, 3, or 4. The calculation is made for a two-dimensional system in which the flow passes through four ramps of equal angles shown schematically in Fig. 2 and described later in detail. The ramp angles are changed arbitrarily until the best specific impulse is obtained. The fuel equivalence ratio is 1.0, and the flow through the nozzle is assumed to undergo a sudden freezing of the main recombination mechanism $OH + H = H_2O$. The detail of the calculation method will be described later. For comparison, the calculation by Billig[2] and the values for a typical hydrogen-oxygen rocket engine are shown. Billig's values are those for which the nozzle flows are calculated kinetically, i.e., accounting for nonequilibrium processes.

As Fig. 1 shows, at 3 km/s the specific impulse values from the three cases are similar. However, at higher speeds the case with the lower M_{ci} gives lower specific impulses. If the combustion entrance Mach number is limited to a fixed value, then it is apparent from Fig. 1 that scramjet propulsion cannot produce a positive thrust beyond a certain flight speed. This is because, at such a high flight speed, in order to maintain the combustion-chamber entrance Mach number to four or below the inlet ramps must be steep. Billig's values are higher than the M_{ci}-unlimited case at low speeds probably because 1) the temperature of the injected fuel is assumed to be as high as 2000 K in his work, whereas it is assumed to be at 500 K in the present calculation and 2) a more efficient inlet compression process is assumed in the work of Billig. At high speeds Billig's values are lower because friction loss is accounted for in his work.

One possible means of alleviating this Mach-number limitation and extending the operating speed of scramjet propulsion system to high Mach numbers is the use of the MHD-bypass scheme.[1,3] If the airflow entering the combustion chamber has an electrical conductivity value above a certain minimum level, then one could

Received 26 November 1999; revision received 8 September 2000; accepted for publication 18 October 2000.

*Senior Research Scientist. Fellow AIAA.
†Senior Research Scientist. Associate Fellow AIAA.
‡Division Scientist, Space Technology Division. Associate Fellow AIAA.

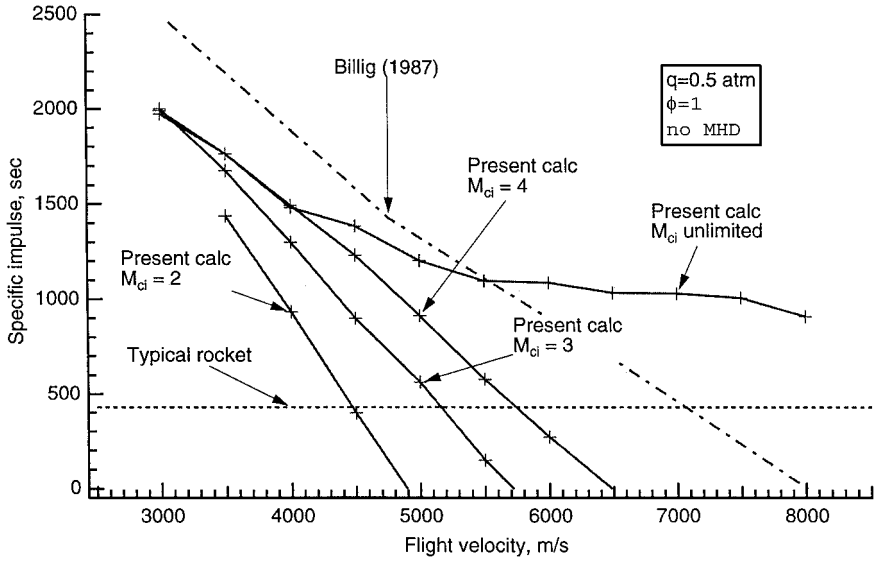

Fig. 1 Comparison between the theoretical specific impulse of a frictionless scramjet, with and without limitation on combustion-chamber entrance Mach number. The calculation (with friction loss and with finite rate chemistry) by Billig[2] is shown also for comparison.

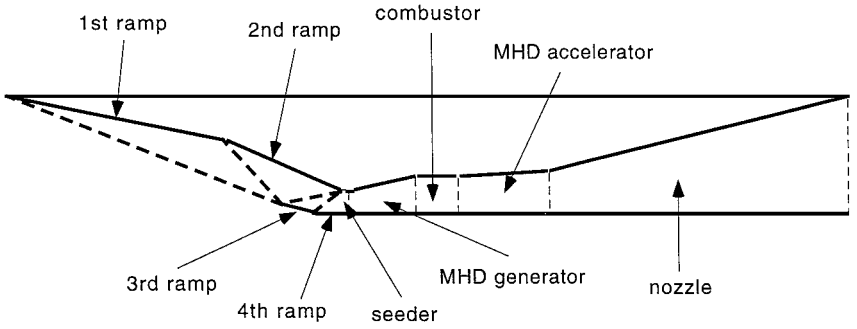

Fig. 2 Schematic of the four-ramp MHD-bypass scramjet system.

conceivably decelerate the flow by the use of an MHD generator to bring down the flow Mach number to the acceptable value. After combustion an MHD accelerator could accelerate the flow using the electrical power produced by the generator. The scheme is shown schematically in Fig. 2. By this approach a portion of the flow energy bypasses the combustion chamber.

For an MHD action to be practical, electrical conductivity must be at least of the order of 50–100 mhos per meter. With an electrical conductivity value below this level, the magnetic field strength and the electrical voltage required for an MHD action become too large to be practical. Electrical conductivity is determined mostly by the degree of ionization. The required level of ionization occurs in air at equilibrium for temperatures above 5000 K. By seeding air with potassium to a mole fraction of about 10^{-3}, the required conductivity can be obtained under equilibrium at about 3500 K. By seeding with cesium, it can be obtained at temperatures as low as 2800 K. (Note that isotopes producing alpha particles for ionizing air are not considered because of the health hazard.)

A possibility exists that the electrical conductivity required for such an MHD device can be obtained under a nonequilibrium condition,[4] instead of the equilibrium condition envisioned in the present work. By adding energy preferentially to electrons by means of an electron beam or intense optical radiation, the electron density could perhaps be made sufficiently high to produce the required electrical conductivity even when the gas temperature is low. Such a system has the potential advantage of enabling MHD action at low flight speeds. Such a system is not considered in the present work because of the uncertainty about the magnitude of the energy required to produce and maintain a high nonequilibrium electron density and about the extent of flow heating produced by this energy addition.

The airflow leaving the inlet in a scramjet system is at an elevated temperature because of the compression in the inlet. If this temperature is 3500 K, for example, then by seeding air with potassium, an MHD-bypass scheme can function. Such a high temperature can occur at flight speeds above about 3000 m/s with relatively steep inlet compression. At higher flight speeds the required temperature can be obtained with a shallower inlet compression angle.

In Fig. 3 the geometry of such an MHD-bypass system is compared with that of a non-MHD system for a flight dynamic pressure of 0.5 atm, velocity of 4500 m/s, fuel equivalence ratio of 1, and a M_{ci} value of 2. As seen here, in order for a non-MHD vehicle to produce M_{ci} of 2, the ramp angles δ must be 21.25 deg. For an MHD-bypass vehicle δ becomes 15.7 deg. Because the MHD-bypass vehicle can now tolerate a higher Mach number at the end of inlet compression than a nonMHD-bypass vehicle, the loss in total pressure will be less, and hence the pressure drag on the inlet will be less. As a result, the inlet drag for the MHD-bypass vehicle becomes less, as will be shown later.

In the present work a theoretical calculation is performed to predict the maximum possible theoretical performance of such an MHD-bypass scramjet system. Assumptions made are the following: 1) the flow is inviscid everywhere; 2) the seed material and fuel are mixed perfectly without producing shock waves or viscous dissipation; 3) the electrical current densities through the MHD devices are uniform at each axial location; and 4) the gas is in thermochemical equilibrium except in the region downstream of the chemical freezing point in the nozzle.

Method of Calculation

The MHD-bypass scramjet system is assumed to be two-dimensional and has a width of 1 m. The inlet compression is achieved through four ramps of equal angles δ, as indicated in Fig. 2. The cowl bends the flow twice and thus forms the third and the fourth ramps, as shown.

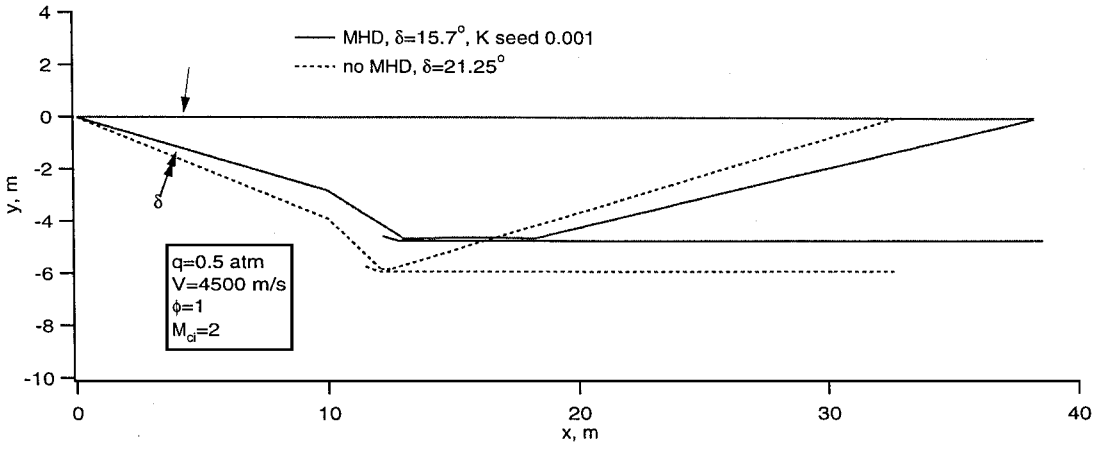

Fig. 3 Comparison of vehicle geometry between an MHD- and non-MHD-bypass scramjet system.

At the end of the fourth compression, seeding is assumed to occur. Liquid potassium or cesium is assumed to be injected into the flow instantly without causing shock waves or viscous dissipation. The flow condition after seeding is calculated by solving the conservation equations for the mass, momentum, and energy.

After seeding the flow enters the MHD generator. In the generator the flow processes are assumed to occur one-dimensionally, i.e., uniformly across the device, under equilibrium, and under a constant load factor $\alpha = E_y/uB$. The value of α for a generator, α_1, is always less than unity. The magnetic field intensity is selected so that deceleration to the desired Mach number is completed within the given lengths of the MHD device.

The governing equations for this one-dimensional flow are[5]

$$\rho u\left(\frac{\mathrm{d}u}{\mathrm{d}x}\right) = -\left(\frac{\mathrm{d}p}{\mathrm{d}x}\right) + jB \tag{1}$$

$$\rho u\left[\frac{\mathrm{d}(h + u^2/2)}{\mathrm{d}x}\right] = jE_y \tag{2}$$

The electrical current density j is given by

$$j = \sigma(E_y - uB) \tag{3}$$

The axial voltage gradient E_x is related to the transverse voltage gradient E_y by

$$E_x = \Omega(E_y - uB) \tag{4}$$

The Hall parameter Ω is a product of the electron cyclotron angular frequency ω and the average collision time τ for electrons

$$\Omega = \omega\tau \tag{5}$$

The cyclotron angular frequency ω is given by $\omega = 1.76 \times 10^{11} \times \mathrm{B\ sec^{-1}}$. By integrating Eqs. (1) and (2) along the streamline, one obtains all flow properties: j, E_x, E_y, and Ω. The requirement of mass conservation yields the required cross-sectional area of the MHD device, which satisfies the constant α requirement. By multiplying E_y by the height of the MHD channel so determined, one obtains the voltage across the electrodes.

The electrical conductivity σ and the average collision time τ are calculated using the method given in Ref. 6 with the collision integrals given therein. For the collisions of neutral potassium or cesium with other species, the collision integrals are estimated from the atomic weights through an interpolation/extrapolation scheme. The accuracy of these collision integrals is not important because the contribution of the neutral seed species to the electrical conductivity is small.

The flow exiting from the MHD generator enters the combustion chamber. Here, gaseous hydrogen fuel is assumed to be mixed instantly without causing any shock waves or viscous dissipation. The fuel is assumed to be pumped (in the liquid form) to a pressure of $2 \times 10^7/\phi$ Pa. The pressure of 2×10^7 Pa, for $\phi = 1$, is chosen considering the fact that it is about 2.5×10^7 Pa for the space shuttle main engines. The division by ϕ accounts for the fact that the pump power remains fixed independently of the ϕ value. The total temperature of the fuel is assumed to be 500 K/ϕ, for the reason given in the Appendix. The division by ϕ here accounts again for the fact that the heat available to the fuel is fixed. The high-pressure fuel is assumed to undergo a supersonic expansion to an area ratio, where the static pressure becomes equal to that of the combustor entrance. The cross-sectional area of the nozzle exit is added to the flowpath cross-sectional area.

The combustion process is calculated assuming equilibrium. The species included in the calculation are O, H, O_2, H_2, NO, OH, H_2O, K (or Cs), and K^+ (or Cs^+). The flow exiting from the combustion chamber enters the MHD accelerator. The flow in the accelerator is calculated by the same method as for the generator. The only difference is that the load factor α_2 is greater than unity for the accelerator.

The flow exiting from the MHD accelerator enters the nozzle. The nozzle is assumed to be linear and two sided as shown schematically in Fig. 2. At the beginning of the nozzle expansion, the flow is assumed to be in thermal and chemical equilibrium. The nozzle flow is calculated by integrating the conservation equations assuming equilibrium. At each point the Damköhler number (the ratio of the flow residence time to chemical reaction time) of the recombination reaction

$$\mathrm{OH + H + M \rightarrow H_2O + M}$$

is calculated. The flow residence time is defined as that time required for the flow to travel the distance that produces cross-sectional area changes of 10%. The chemical reaction time is defined as that time required for this recombination reaction to produce a 10% change in the concentration of OH, O, and H_2O. Initially, the ratio of the two times is greater than unity, and it then decreases with x. When the Damköhler number becomes unity, the chemical reaction is assumed to freeze. The reaction rates needed in this calculation are obtained from Ref. 7. After freezing the process is taken to be isentropic expansion with specific heat ratio calculated at every point.

The thrust is calculated as the difference between the outgoing (at the tail of the vehicle) and incoming momenta (at the nose of the vehicle), accounting for the presence of the deflection at the leading edge of the cowl (see Fig. 2). Specific impulse is calculated by dividing this thrust by the sum of the flow rates of the fuel and the seed material. The overall MHD-bypass performance of the system is represented by the energy bypass ratio:

$$\text{Energy bypass ratio} = \text{Enthalpy extraction ratio}$$

$$= \frac{\text{Electric power transferred}}{\rho u H A \text{ at generator entrance}}$$

$$= \frac{\rho u H A \text{ at generator entrance} - \rho u H A \text{ at gen. exit}}{\rho u H A \text{ at generator entrance}} \tag{6}$$

The changes in kinetic energy flow $0.5\rho u^3 A$ in both generator and accelerator are equal to this electrical power transferred. The ohmic ($\boldsymbol{j}\cdot\boldsymbol{E}$) loss (joule heating) produces an increase in entropy S and consequently a decrease in the possible isentropic expansion work, which could be transformed into kinetic energy of the flow. This loss of available energy for the system (joules per second) is

$$\text{loss} = \rho u A \int T\,\mathrm{d}S \tag{7}$$

This loss is proportional to $1-\alpha_1$ in the generator. Thus, the loss is

$$\text{loss} = (\text{electric power transferred}) \times (1-\alpha_1) \tag{8}$$

Likewise, in the accelerator

$$\text{loss} = (\text{electric power transferred}) \times \left(\frac{\alpha_2 - 1}{\alpha_2}\right) \tag{9}$$

By writing out the equations of motion in an MHD device, one can show that the loss of available energy appears as a pressure drop in the device (generator or accelerator). The total loss becomes

$$\text{total loss} = (\text{electric power transferred}) \times \left[(1-\alpha_1) + \left(\frac{\alpha_2 - 1}{\alpha_2}\right)\right] \tag{10}$$

Implicit in this statement is the tacit assumption that the power loss in the electrical system by ohmic heating is zero.

Parameter Specification

The length of the first ramp is assumed to be 10 m. The length of the combustion chamber is assumed arbitrarily to be 0.4633 m. The maximum allowed length of the MHD generator is set arbitrarily to 2.721 m, whereas that of the accelerator is set to 2.846 m. The length of the nozzle is set arbitrarily to 20.23 m. The flight dynamic pressure $q = \rho V^2/2$ is varied between 0.25 and 1.0 atm. The fuel equivalence ratio is varied between 1 and 2. The load factor E_y/uB is varied: for the generator it is between 0.8 and 0.95; for the accelerator it is between 1/0.95 and 1/0.8. The seeding mass fraction is varied between 10^{-3} to 3×10^{-3}. The freestream temperature is assumed to be 250 K. The combustor entrance Mach number M_{ci} is varied between 2 and 4. The flight speed is varied from 3 to 8 km/s. The ramp angles are varied from 3 to 25 deg.

Table 1a Summary of a typical solution (Figs. 4a–4f): Compression stage

Flow variable	Freestream	First ramp	Second ramp	Third ramp	Fourth ramp
Velocity, m/s	4500	4229	3925	3597	3244
Temperature, K	250	1566	2454	3083	3592
Pressure, Pa	3.607e2	1.005e4	5.246e4	1.864e5	5.359e5
Mach number	14.45	5.320	4.644	3.741	3.077

If the MHD devices are long, the flow therein can become separated. Though there are no data on this phenomenon, it is probably prudent to take the ratio of the length to the diameter of the MHD devices to be not more than 20. As will be seen later, the height of the MHD devices in the present two-dimensional calculation is of the order of a few centimeters. This implies an allowed length of MHD devices of only about 1 m. However, if a three-dimensional compression were to be used, the MHD devices may have a square cross section of, e.g., 30×30 cm. Such a device may have an allowable length of 6 m. With this possibility available no effort is made in the present work to justify the arbitrarily set lengths of the MHD devices.

Flowpath Behavior

In Figs. 4a–4f and Table 1 a typical result is shown. For this case the flight velocity is 4.5 km/s, and the angle of all four ramps is 15.7 deg. The overall inlet area ratio is 70.65. The load factors are $\alpha_1 = 0.95$ for the generator and $\alpha_2 = 1/0.95$ for the accelerator. The combustor entrance Mach number is 2, and the equivalence ratio ϕ is 1. The total temperature and the total pressure of the fuel are, respectively, 500 K and 2×10^7 Pa. The velocity of the fuel injector nozzle exit is 3084 m/s. The mass fraction of the potassium seed is 10^{-3}. The geometry of the vehicle is that shown in Fig. 3. This particular design consumes hydrogen fuel at a rate of 3.042 kg/s and potassium at a rate of 0.1030 kg/s (3.39% of fuel).

As Figs. 4a–4d and Table 1a show, from the first ramp to the fourth ramp pressure and temperature rise, and velocity and Mach number fall as expected. Seeding produces virtually no change in thermodynamic conditions because the amount of seed is small. The MHD generation reduces the pressure, velocity, and Mach number, as expected. In the combustor the pressure and temperature rise (from 4.636×10^5 to 7.017×10^5 Pa and from 3576 to 3622 K), and the velocity and Mach number fall (Table 1b). In the MHD accelerator the pressure falls, but the velocity and Mach number rise.

One noticeable feature of the solution (see Table 1b) is that the height of the flowpath channel is small: it is 6.47 cm at the entrance to the seed chamber and 7.86 cm at the entrance to the nozzle. Such small heights would result in a laterally elongated cross section of the channel resulting in a large surface area and hence a large friction loss. In the MHD devices such an elongated cross section would result in a very difficult magnetic field arrangement: there is no space for the return path of the magnetic field. This difficulty is a result of the assumption of two-dimensionality. In a real flight vehicle this would be avoided by compression in the third dimension. Hence, no attention is paid in the present work to the awkward appearance of the flow path.

One consequence of the unrealistically small height of the flowpath is the low voltage developing across the opposing electrodes (Fig. 4e): it is only 1596 V at the entrance of the MHD generator and 2427 V at the exit of the accelerator. A wider flowpath will produce a corresponding larger voltage across the electrodes. In Fig. 4f and Table 1b the negative values of transverse voltage gradient and electrical current in the MHD generator occur because

Table 1b Summary of a typical solution (Figs. 4a–4f): MHD

Quantity	Generator entrance	Generator exit	Accelerator entrance	Accelerator exit
Height, cm	6.473	11.50	11.65	7.86
Length, m	——	2.696	——	2.394
B field, T	8.010	8.010	9.559	9.559
Hall parameter	4.056	4.681	3.183	3.510
Transverse E, V/m	−24,650	−16,020	18,850	30,850
Axial E, V/m	5,000	3,974	3,000	5,415
Voltage across electrodes, V	1,596	1,843	2,196	2,427
Current density, A/m2	−9.160e4	−6.161e4	4.319e4	7.139e4
Velocity, m/s	3,240	2,102	1,873	3,066
Mach number	3.072	2.000	1.538	2.522
Ionization mole fraction	——	9.739×10^{-5}	7.799×10^{-5}	——
Electrical conductivity, mho/m	——	70.58	45.83	——

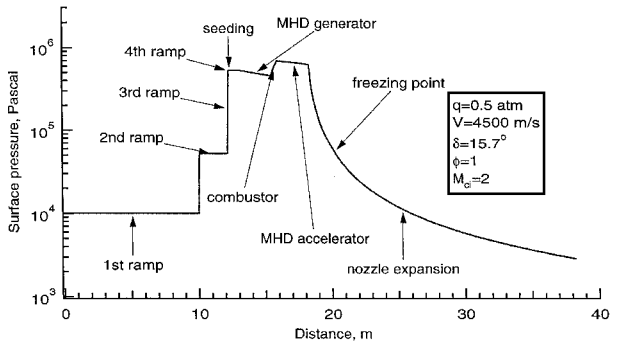

a) Pressure

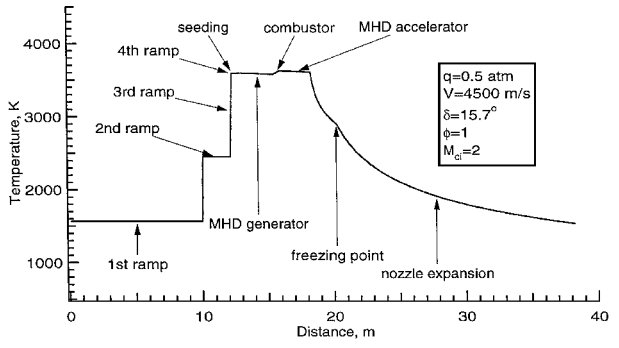

b) Temperature

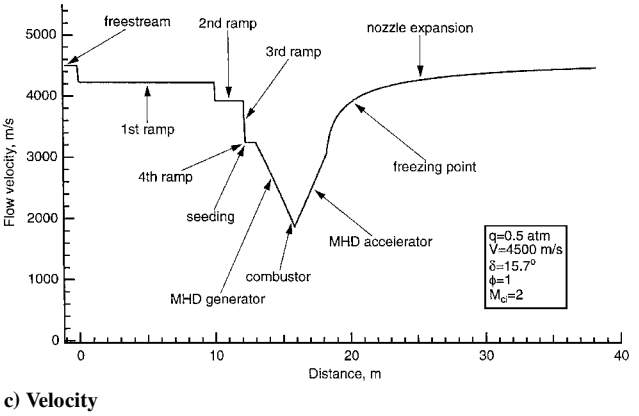

c) Velocity

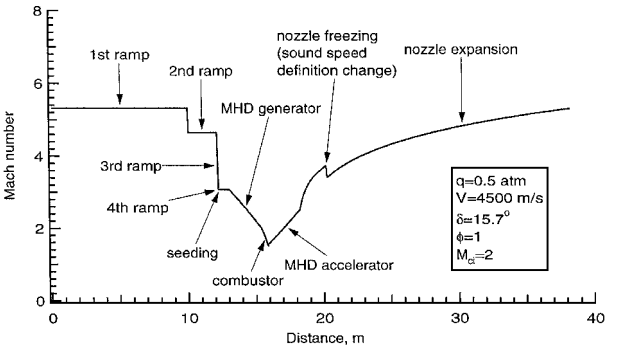

d) Mach number

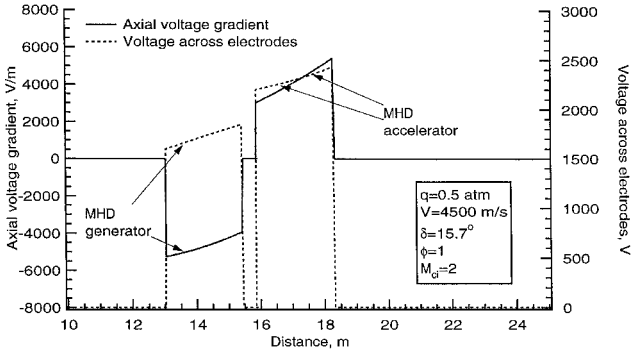

e) Axial voltage gradient and voltage across electrodes

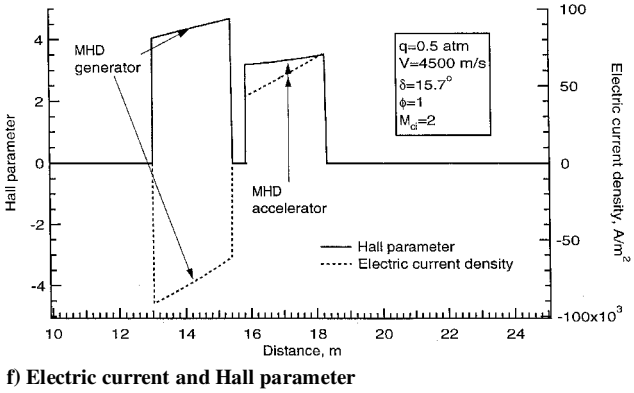

f) Electric current and Hall parameter

Fig. 4 Behavior of the flow through the flowpath: V = 4.5 km/s, q = 0.5 atm, ramp angles δ = 15.7 deg, α_1 = 0.95, α_2 = 1/0.95, M_{ci} = 2, and ϕ = 1.

the current is flowing in the direction opposite to that in the MHD accelerator.

In the nozzle sudden freezing occurs at a Mach number, a velocity, a temperature, and a pressure of 3.73, 3919 m/s, 2907 K, and 5.605×10^4 Pa, respectively. At the freezing point the molar concentrations of O, H, and OH are relatively small, i.e., 1.52×10^{-2}, 4.03×10^{-2}, and 3.95×10^{-2}, respectively. This indicates that a substantial portion of the combustion energy is recovered in the nozzle expansion prior to freezing. Molar concentrations of O_2, H_2, NO, H_2O, and K^+ are, respectively, 1.98×10^{-2}, 6.61×10^{-2}, 1.17×10^{-2}, 0.2133, and 4.03×10^{-5}. The nozzle exit velocity (4492 m/s) is slightly smaller than the flight velocity because of the losses by inlet compression and by MHD processes. The positive thrust is produced mostly by the increase in the mass flow rate (caused by fuel injection) and to some extent by the high static pressure at the nozzle exit (2.845×10^3 Pa). The area ratios at the freezing point and at the nozzle exit are, respectively, 7.008 and 60.2.

The electrical power transferred from the generator to the accelerator equals exactly the changes in the kinetic energies in these devices. With the energy bypass ratio being 0.2926, according to Eq. (6) 0.2926 of the flow energy $\rho u H A$ is taken away in the generator as the electrical power and later put back in the accelerator. The total (sum of generator and accelerator) loss of available energy for conversion to kinetic energy later in the nozzle, given by Eq. (10), is $0.05 + 0.05 = 0.1$ of the electrical power transferred and hence 0.02926 of the flow power, $\rho u H A$. The overall performance in terms of net thrust and specific impulse is 2.641×10^4 N and 856.2 s, respectively.

In Fig. 5 the pressure distribution for the calculated MHD-bypass vehicle is compared with that for a non-MHD-bypass vehicle subject to the same constraint $M_{ci} = 2$. For the non-MHD-bypass vehicle the ramp angle is $\delta = 21.25$ deg, whereas the angle is 15.7 deg for the MHD-bypass vehicle. The geometries of these vehicles were shown in Fig. 3. In Fig. 5 the location of the end of the four ramp-compressions is indicated for the two vehicles. Upstream of this demarcation point, pressure produces drag; in the downstream, pressure produces thrust. For the MHD-bypass vehicle the drag-producing pressure is lower than that for the non-MHD-bypass vehicle because of the smaller δ. This is the reason why the MHD-bypass vehicle attains a higher specific impulse. The specific impulse is 856.2 s, which is nearly twice that of the typical rocket engine, 430 s, and which is more than twice that of the non-MHD-bypass vehicle, 398.8 s.

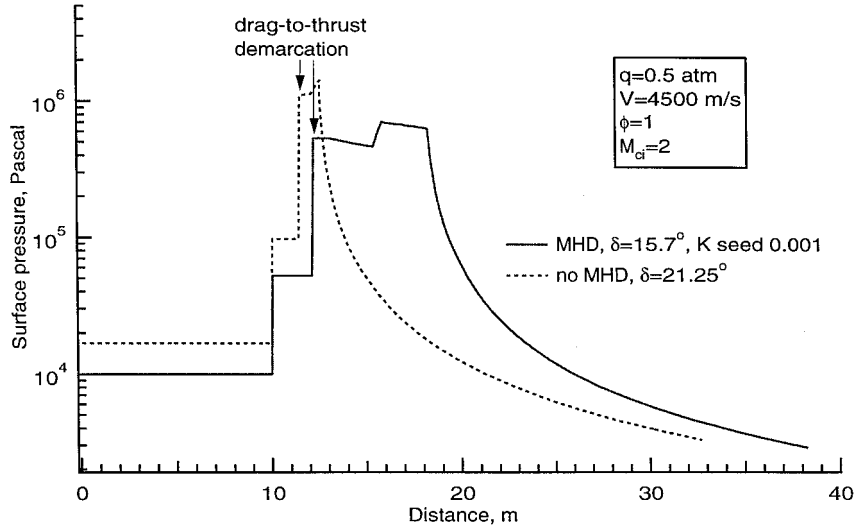

Fig. 5 Comparison between the pressure distribution for MHD-bypass and non-MHD-bypass vehicles.

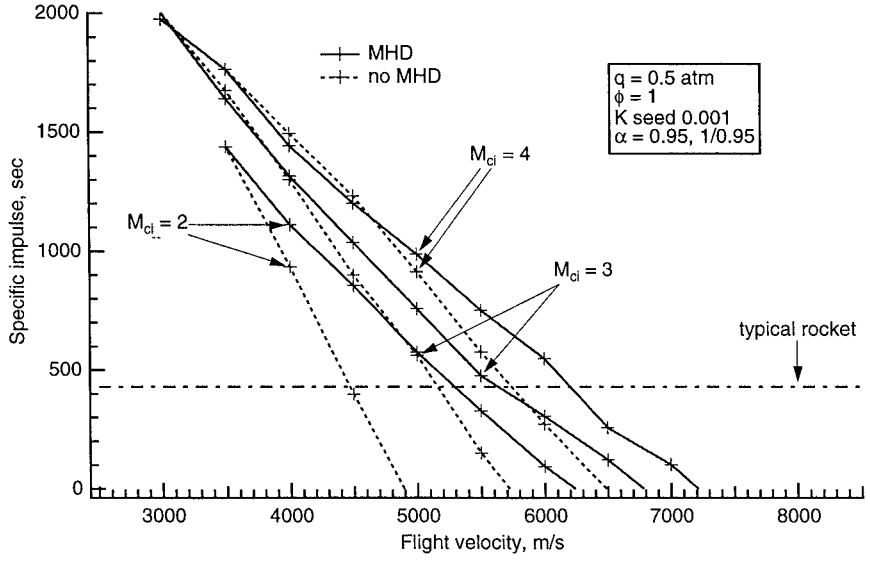

Fig. 6 Comparison of specific impulses between MHD and non-MHD cases.

Parametric Study

For any flight speed the specific impulse varies with the ramp angle given. The highest specific impulse value is chosen by searching through the solutions for a range of ramp angle values.

In Fig. 6 the highest specific impulse values obtained at each given flight velocity for the MHD-bypass scramjet system are compared with those for the non-MHD-bypass system. As seen in the figure, up to a flight speed of about 3500, 4000, and 4500 m/s, respectively, for $M_{ci} = 2$, 3, and 4, there is not much difference in the specific impulses attained between the MHD and non-MHD cases. Above those speeds the specific impulse values for the MHD case are appreciably higher than those for the non-MHD system. Between 3500 and 5300 m/s the specific impulses with MHD for $M_{ci} = 2$ are higher than the rocket value, whereas, for $M_{ci} = 4$ the MHD system remains superior to the rocket up to 6200 m/s.

In Fig. 7 the effect of flight dynamic pressure q on specific impulse is shown for $V = 4500$ m/s, $M_{ci} = 2$, and potassium seeding of 0.001 by mass. As seen here, specific impulse improves slightly as q is increased for both MHD-bypass and non-MHD-bypass cases. This is because, as pressure in the flowpath increases, the degree of dissociation under equilibrium decreases and the freezing in the nozzle occurs later so that more chemical energy is recovered into the flow kinetic energy in the nozzle.

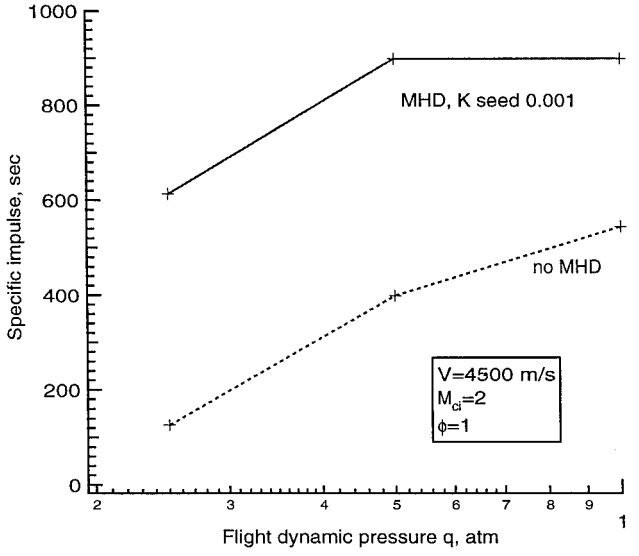

Fig. 7 Effect of flight dynamic pressure on specific impulse: V = 4.5 km/s, M_{ci} = 2, α_1 = 0.95, and α_2 = 1/0.95.

In Fig. 8 the effect of fuel equivalence ratio on specific impulse ϕ is shown. The ϕ value is varied between 1 and 1.5 for the MHD case. At higher ϕ values choking occurs for the MHD case. As seen here, specific impulse improves as ϕ is increased. In Table 2 conservation of energy is checked. The energy flows at the nozzle exit for both $\phi = 1$ and 1.5 are below the theoretical available energy flow values. The energy loss is caused by chemical losses associated with incomplete recombination. Therefore, energy conservation is satisfied. The increase in specific impulse for $\phi = 1.5$ is caused by the increase in the mass flow rate at nozzle exit and to the lower combustor exit temperatures and to reduced dissociation.

In Fig. 9 the specific impulses are compared between the cases where the seeding material is potassium and cesium, the seed mass fraction being 0.001 for potassium and 0.003 for cesium. The mass fraction must be higher for cesium because cesium is heavier. The figure shows that potassium seed is slightly better.

Table 2 Energy flow tally

Quantity	$\phi = 1$	$\phi = 1.5$
Airflow rate entering combustor, kg/s	102.98	102.98
Energy in flow entering combustor, J/s	1.0686×10^9	1.0686×10^9
H_2 flow, kg/s	3.042	4.563
Available chemical energy, J/s	3.647×10^8	3.647×10^8
Available energy at combustor exit, J/s	1.433×10^9	1.433×10^9
Calculated nozzle-exit energy, J/s	1.316×10^9	1.394×10^9

In Fig. 10 the effect of varying the load factors α_1 and α_2 is shown. As the figure shows, the specific impulse is a strong function of the α. The closer the α to unity, the higher becomes the specific impulse. This is because the electrical energy converted to heat increases as α deviate from unity, as indicated by Eqs. (8) and (9). This leads to increased pressure losses and lower efficiency.

Discussion

The present calculation shows encouraging results for the MHD-bypass scheme. The shortcomings of the present work are the neglect of the three-dimensionality of the flow in the MHD devices and of the viscous losses. Accounting for the three-dimensionality and the viscous losses are the next step in this line of investigation.

In the present work the MHD devices were assumed to be of Faraday type. Such devices have a drawback that the electrical circuits supplying and extracting power to and from the MHD devices are complicated. This complexity can be avoided by changing the design to the diagonally connected generator/accelerator loading configuration. All other operating parameters will remain unchanged from those of the present Faraday design.

One interesting observation of the present solutions concerns the axial voltage gradient. As shown in Fig. 4e, the axial voltage gradients are ~5000 V/m or less. Two electrodes separated by an insulator are known to start arcing between them if the voltage difference between them exceeds about 50 V. In MHD devices built in the past for terrestrial use, the electrodes typically had widths of

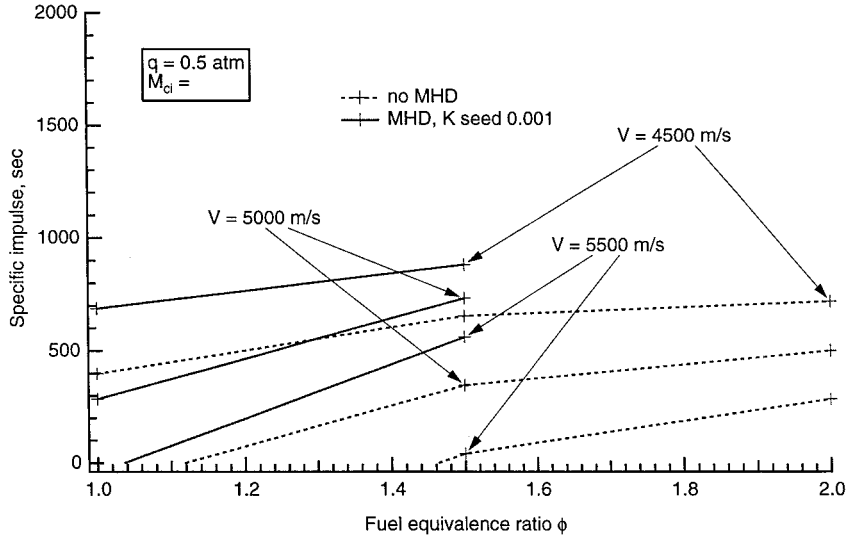

Fig. 8 Effect of equivalence ratio ϕ on specific impulse: $\alpha_1 = 0.95$ and $\alpha_2 = 1/0.95$.

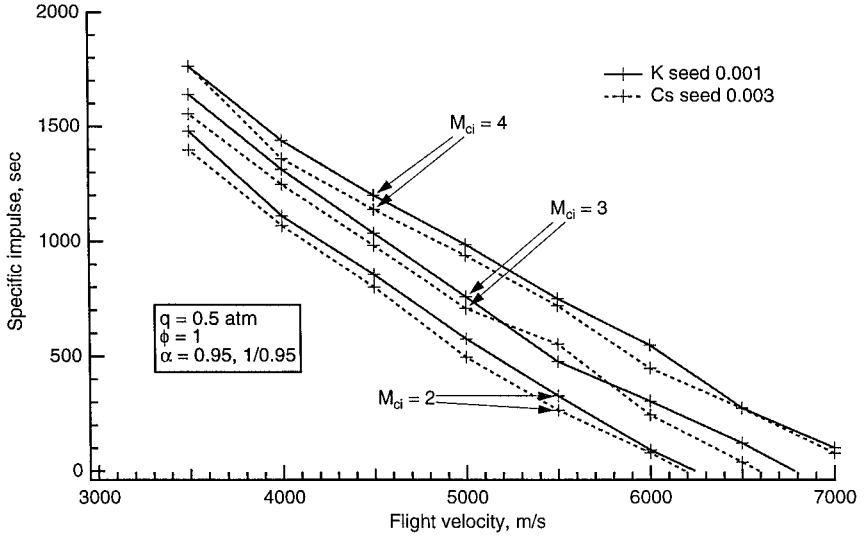

Fig. 9 Comparison between potassium and cesium seeding: $q = 0.5$ atm, $\phi = 1$, $\alpha_1 = 0.95$, and $\alpha_2 = 1/0.95$.

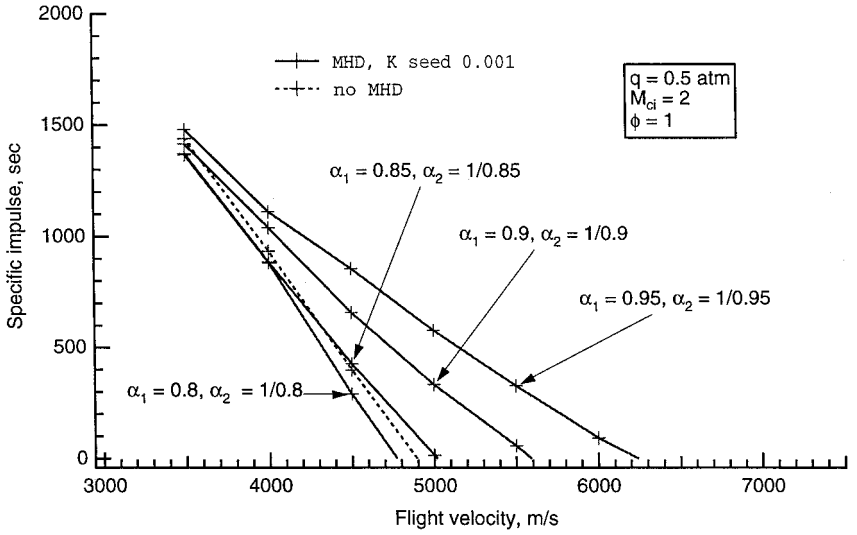

Fig. 10 Effect of varying the load factors α_1 and α_2.

about 1 cm, resulting in the axial voltage gradient limit of about 5000 V/m. The MHD system considered in the present work does not exceed this voltage gradient limit.

The voltage gradients required in the present scheme are much lower than those that would be required by a system using nonequilibrium ionization such as that proposed in Ref. 3. Nonequilibrium ionization schemes produce electrical conductivities that are at least one order of magnitude less than the equilibrium ionization values achieved in the present scheme. To pass the same electrical current density with this low electrical conductivity, the voltage gradient must be very large, greatly exceeding the 5000 V/m limit. This is one major difficulty in realizing the MHD-bypass scheme relying on nonequilibrium ionization.

The technologies associated with MHD have been developed in the past few decades. As a result, the technologies of seeding and those of power generation are both well developed. However, the technology of acceleration is relatively less developed. Research and development must be carried out on the technology of MHD acceleration before the feasibility of an MHD-bypass system can truly be assessed. Additionally, light-weight 8-T magnets are still years away from reality. Research and technology development are also needed to address this issue.

Conclusions

If supersonic combustion is possible only at combustor-entrance Mach numbers below a fixed value, then the MHD-energy-bypass system can enhance the performance of scramjet propulsion at high flight speeds by virtue of slowing down the flow entering the combustor. Consequently, the MHD-bypass system can extend the operational range of a spaceliner with conventional scramjets. In other words, the MHD system can delay the firing of the rocket engine for insertion of the single-stage-to-orbit spaceliner in low Earth orbit.

For a frictionless system with a load factor of 0.95, the MHD-bypass system can produce a specific impulse better than a typical rocket system to a flight speed of about 6 km/s. Performance is better for a higher flight dynamic pressure and higher combustor inlet Mach number, but is degraded greatly as the load factor moves away from unity.

Appendix: Estimation of Fuel Temperature

A hypothetical scramjet vehicle of 1 m width flying at a speed of 4500 m/s, with its fuel tank nearly empty, is assumed to have a mass of 5×10^4 kg. Its lift force must balance its weight, which is $9.8 \times 5 \times 10^4 \approx 5 \times 10^5$ N. The lift-to-drag ratio of the vehicle is assumed to be 5. Then the drag force is $5 \times 10^5/5 = 10^5$ N. Flying at 4500 m/s, its drag work is $4500 \times 10^5 = 4.5 \times 10^8$ J/s. Assuming that friction drag is $\frac{1}{3}$ of the total drag, the friction work is $4.5 \times 10^8/3 = 1.5 \times 10^8$ J/s. Of this friction work, according to the theory for a highly cooled wall, $\frac{1}{2}$ enters into the skin as heat, which is $1.5 \times 10^8/2 = 7.5 \times 10^7$ J/s. Assuming 30% of this skin-heating energy is captured and used to heat hydrogen fuel, the energy available for heating the fuel is $0.3 \times 7.5 \times 10^7$ J/s $= 2.25 \times 10^7$ J/s. The rate of fuel injection for the case of equivalence ratio of unity is calculated in the present work to be about 3 kg/s. Therefore, the enthalpy rise in the fuel by the addition of this heat is $2.25 \times 10^7/3 = 7.5 \times 10^6$ J/kg. Because the specific heat of the hydrogen fuel is 1.409×10^4 J/(kg-K), the temperature rise in the hydrogen fuel caused by the rise in enthalpy is $7.5 \times 10^6/1.409 \times 10^4 = 532$ K.

Acknowledgment

C. Park and D. W. Bogdanoff wish to acknowledge the support provided by NASA Ames Research Center through Contract NAS2-99092 to Eloret Corporation.

References

[1]Novichkov, N., "At Hypersonic Speeds (In the Large Scale Plan)," Foreign Aerospace Science and Technology Center, FASTC-ID(RS)T-0972-92, Wright–Patterson AFB, Ohio, Jan. 1993 (translated from *Ekho Planety*, Vol. 42, No. 237, Oct. 1992, pp. 4–8).

[2]Billig, F. S., "Current Problems in Non-Equilibrium Gas Dynamics—Scramjet Engines," *AIAA Professional Study Seminar on Non-Equilibrium Gas Dynamics*, Honolulu, Hawaii, June 1987.

[3]Bityurin, V. A., Lineberry, J. T., Potebnia, V. G., Alferov, V. I., Kuranov, A. L., and Sheikin, E. G., "Assessment of Hypersonic MHD Concepts," AIAA Paper 97-2393, June 1997.

[4]Macheret, S., "Electron Beam Generated Plasmas in Hypersonic MHD Channels," AIAA Paper 99-3635, June 1999.

[5]Jahn, R. G., *Physics of Electric Propulsion*, McGraw–Hill, New York, 1998, p. 203.

[6]Yos, J. M., "Transport Properties of Nitrogen, Hydrogen, Oxygen, and Air to 30,000° K," AVCO, Research and Advanced Development Division Technical Memorandum RAD TM-63-7, AVCO-RAD, Wilmington, MA, March 1963.

[7]Oldenborg, R., Chinitz, W., Friedman, M., Jaffe, R., Jachimowski, C., Rabinowitz, M., and Schott, G., "Hypersonic Combustion Kinetics," Status Rept. of the Rate Constant Committee, NASP High Speed Propulsion Technology Team, Dec. 1989.